

Lattice Vibrations of Semiconductors with a Defect Zinc-Blende Structure*

E. Finkman and J. Tauc

Division of Engineering and Department of Physics, Brown University, Providence, Rhode Island 02912

(Received 9 July 1973)

We report infrared spectra of defect-structure cubic compounds In_2Te_3 , Ga_2Te_3 , and Ga_2Se_3 . The spectrum of In_2Te_3 with ordered vacancies is analyzed using sixfold folding of the first Brillouin zone of the zinc-blende structure in the [110] and [111] directions. It is shown that both folding models describe well the observed structure of the spectra of In_2Te_3 with ordered or disordered vacancies.

Cubic $A_2^{\text{III}}B_3^{\text{VI}}$ compounds are characterized by a crystal structure based on a tetrahedral atomic coordination as in the zinc-blende structure. However, one third of the cation sites available to A atoms are vacant. These compounds represent an interesting case of solids with completely satisfied chemical bonds but with a very large concentration of vacancies.¹ Furthermore, the vacancies may exist in an ordered or disordered state in the same material (e.g., in the α and β phases of In_2Te_3 , respectively). Finally, these materials remain semiconducting even after melting.^{2,3} Although experimental work has been done on the structural,⁴⁻⁷ electrical,⁸ and optical⁹ properties of these compounds, in particular on In_2Te_3 , no work on lattice vibrations has been published.

We report here measurements of the infrared and Raman spectra of polycrystalline α - and β - In_2Te_3 and of polycrystalline partially ordered Ga_2Te_3 and Ga_2Se_3 compounds,¹⁰ carried out in order to study the changes in lattice vibrations induced by a large concentration of ordered and disordered defects introduced into the zinc-blende structure.

Infrared reflection spectra $R(\nu)$ at nearly normal incidence were measured at room temperature with a Digilab Fourier spectrometer, model FTS 14. Infrared transmission spectra measured with powdered samples gave results consistent with those obtained from the reflection measurements. Raman spectra of the tellurides consisted mostly of lines characteristic of crystalline Te, which were found even when the excitation power was low and the surfaces were freshly cleaved. Raman spectra of Ga_2Se_3 measured on polycrystalline samples were consistent with the infrared data. We intend to make a detailed Raman study of Ga_2Se_3 when good single crystals are available.

Infrared reflection spectra (Fig. 1) of disor-

dered structures show two strong *Reststrahlen* bands, each of which is split in the ordered structure. In the low-energy range several weaker bands are observed in α - In_2Te_3 . The low-energy bands are smeared out in the disordered structures; they are too weak for a detailed analysis.

The dielectric constant $\epsilon = \epsilon_1 + i\epsilon_2$ was constructed as a superposition of Lorentzian oscillators:

$$\epsilon(\nu) = \epsilon_\infty + \sum_j \frac{S_j \nu_j}{\nu_j^2 - \nu^2 - i\gamma_j \nu_j \nu}. \quad (1)$$

Initial parameter values were found from a Kramers-Kronig analysis of $R(\nu)$. The reflection spectra were then fitted with a standard deviation of 1% by an iterative computer program. The oscillator parameters thus determined for ordered In_2Te_3 are given in Table I, and the calculated ϵ_2 is in Fig. 2.

A direct theoretical approach to classify the vibrational modes seems not only difficult but

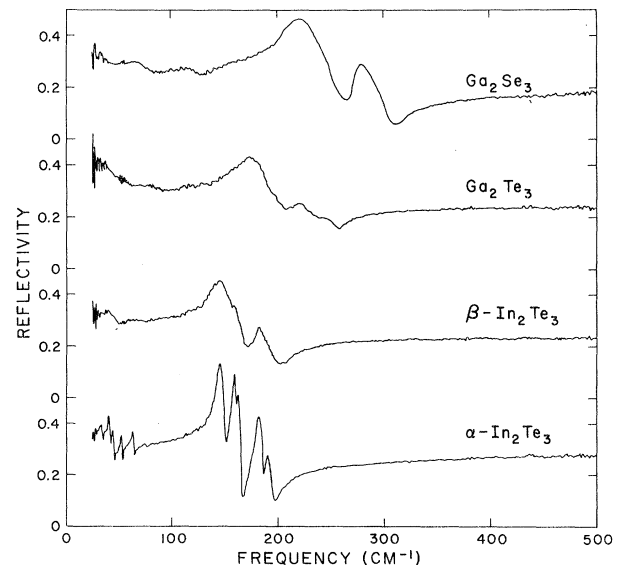


FIG. 1. Reflection spectra for several $A_2^{\text{III}}B_3^{\text{VI}}$ cubic compounds; spectral slit width is 2 cm^{-1} .

TABLE I. Oscillator parameters for α -In₂Te₃.

ν_j (cm ⁻¹)	s_j	γ_j
32.9	0.288	0.044
40.0	0.504	0.046
43.5	0.417	0.054
51.8	0.124	0.010
63.0	0.189	0.030
74.0 ^a		
145.3	1.412	0.031
157.7	0.664	0.026
162.0	0.066	0.011
181.9	0.359	0.025
191.3	0.167	0.033
$\epsilon_\infty = 10.1$ ^b		

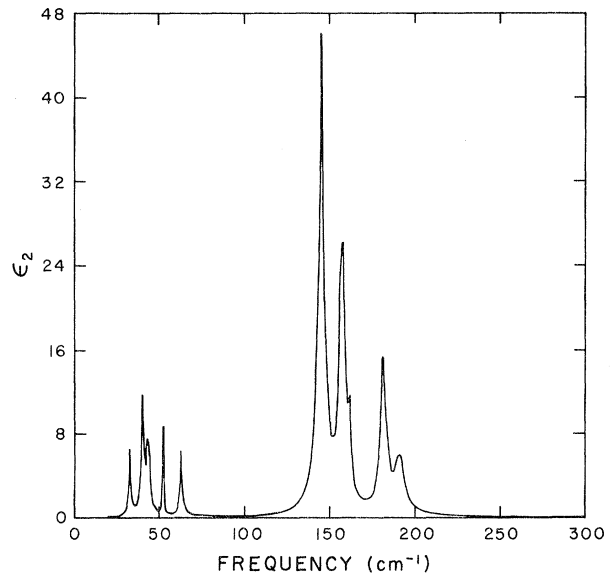
^aThis line is very weak; its position was determined from transmission data.

^bInterference pattern in the transmission data of a thin plate around 1000 cm⁻¹ gave a value $\epsilon_\infty = 10.3$.

perhaps also of little practical significance. The unit cell of the ordered structure contains a very large number of atoms, and the vibrational modes are expected to have many degeneracies and overlaps. However, the simplicity of the infrared spectra suggests that the basic structure of the phonon spectra can be understood if we consider the relation of the crystal structure of the α phase to the zinc-blende (zb) structure.

There has been some controversy⁶ on the structure of α -In₂Te₃ which, however, appears to have been resolved⁷ in favor of the fcc structure with the space group $F\bar{4}3m$. The unit cell consists of 27 zb cubic cells and contains 108 Te and 72 In atoms, and 36 vacancies. Each In atom always has four Te nearest neighbors, while the Te atoms arranged in a fcc structure may have some vacancies as nearest neighbors. We assumed that a Te atom must have at least one In nearest neighbor and constructed the ten fcc structures compatible with this assumption. A striking feature of these models is the uninterrupted straight lines of In atoms which extend through the whole crystal. These lines are always directed along the [110] direction and form a superlattice which is oriented in this direction and has the periodicity of the large unit cell.

The lattice constant of the ordered In₂Te₃ primitive cell is 6 times larger than that of the primitive cell of the zb structure. Therefore, the linear dimensions of the first Brillouin zone of α -In₂Te₃ ("real BZ") are 6 times smaller than those

FIG. 2. Imaginary part of ϵ for α -In₂Te₃.

of the zinc-blende structure ("large BZ"). To interpret the spectra we shall use the large BZ instead of the real one. The reciprocal-lattice vectors in the zb structure are $(4\pi/a)(n_1, n_2, n_3)$, in the real structure $(2\pi/3a)(n_1, n_2, n_3)$. Some points inside the large BZ and on its boundaries coincide with some reciprocal-lattice points of the "real" structure. These points are equivalent to the $\vec{k}=0$ point in the real structure, and therefore can be optically active in the first order. This "folding" may generate absorption bands in addition to the Γ modes already present in the zb structure. We assume that the dominant modes can be associated with the modes obtained by folding. The simplicity of the spectra points out that only a small number of the folded modes are strong enough to be observed. We propose two models based on two different assumptions, which may explain why some folded modes are stronger than others:

(a) Structural considerations mentioned above suggest that the modes propagating in the [110] direction dominate the spectrum. The symmetry in this direction is C_s , the branches are singlets, and the transitions are allowed, except for the highest energy point at $\vec{k}=0$ which is longitudinal. The points $(2\pi/a)(1, 1, 0)$ are outside the large BZ and are discarded.¹¹ The two TO branches are assumed to nearly coincide, as is often the case in the [110] direction in materials with zb structures.¹² The points which are folded into $\vec{k}=0$ in the real zone are those with $\vec{k}=(2\pi/a)$

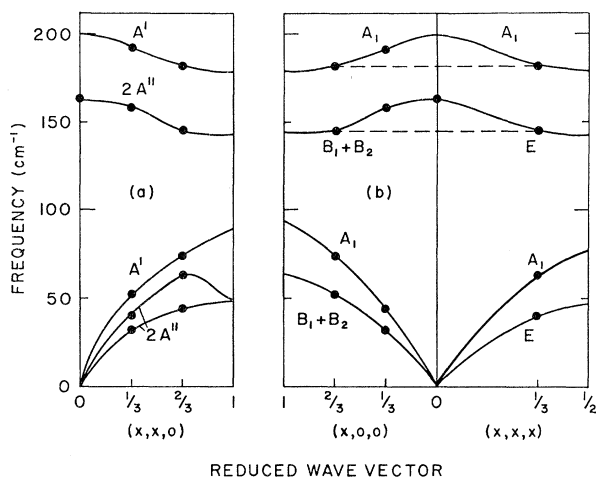


FIG. 3. Schematic phonon dispersion curves for α - In_2Te_3 in the large BZ ($x = 2\pi/a$). Closed circles indicate the observed optical modes; the curve labels indicate the irreducible representations of the symmetry groups discussed in the text. (a) [110] direction, (b) [100] and [111] directions.

$\times (\frac{1}{3}, \frac{1}{3}, 0)$ and $(2\pi/a)(\frac{2}{3}, \frac{2}{3}, 0)$. A possible assignment for the experimentally observed frequencies is shown in Fig. 3(a).

(b) The strongest contributions to the spectrum will come from points which are critical points in the zb structure. With this assumption we have to consider¹³ only [100] and [111] directions since no other critical points are folded into Γ . In the [111] direction the symmetry is C_{3v} . All modes which are not purely longitudinal can be optically active. Only the points $(2\pi/a)(\frac{1}{3}, \frac{1}{3}, \frac{1}{3})$ are inside the large BZ. In the [100] direction the symmetry is C_{2v} (the B_1 and B_2 modes are degenerate because of time-inversion symmetry¹³). All the modes can be optically active. A possible assignment of the observed modes is shown in Fig. 3(b). We assumed that the frequencies of the modes connected with dashed lines are so close that they are not resolved.

We do not have any strong reasons for preferring one model to the other. The analysis of model (a) does not depend on the cubic symmetry of α - In_2Te_3 which has been contested in some papers.^{6, 14, 15} The noncubic structural models discussed by Newman¹⁶ also have straight lines of In atoms extending through the whole crystal in the [110] direction, a feature which we consider essential for the applicability of our arguments.

Both models of the lattice vibrations are consistent with the spectra observed for disordered

In_2Te_3 (β phase). The two strong high-frequency bands we observed are approximately determined by the density of vibrational states. They are peaked at 145 and 180 cm^{-1} , corresponding to the zone-boundary frequencies of the two resolved optic branches in Fig. 3, where the densities of vibrational states are expected to be near a maximum.

It is remarkable that this simple approach describes consistently the observed infrared-active vibrational frequencies of a rather complicated structure. We note that this case is different from that of polytypes of SiC¹⁷ in regard to the relative strength of the additional absorption bands induced by folding. The effect of folding is associated with site inequivalency. Because this is small in the case of SiC, the additional absorption lines are weak. In In_2Te_3 and related "defect" semiconductors the vacancies produce a strong inequivalency. Therefore the additional infrared-active vibrational bands are comparable in strength to the normal TO bands associated with the vibration of Te and In sublattices relative to each other.

We thank Professor A. Wold and Mr. R. Kershaw for the preparation of the materials.

*Work supported by a grant from the National Science Foundation. It has also benefitted from the general support by the National Science Foundation of Materials Science at Brown University.

¹There are many other compounds with ordered or disordered cation vacancies; cf. H. Krebs, *Fundamentals of Inorganic Crystal Chemistry* (McGraw-Hill, London, 1968); M. Robbins and M. S. Miksovsky, *Mater. Res. Bull.* **6**, 359 (1971).

²V. P. Zhuze and A. I. Shelykh, *Fiz. Tverd. Tela* **7**, 1175 (1965) [*Sov. Phys. Solid State* **7**, 942 (1965)].

³W. W. Warren, Jr., *Phys. Rev. B* **3**, 3708 (1971).

⁴H. Hahn and W. Klinger, *Z. Anorg. Chem.* **260**, 97 (1949); H. Hahn, *Angew. Chem.* **64**, 203 (1952).

⁵H. Inuzuka and S. Sugaike, *Proc. Jap. Acad.* **30**, 383 (1954).

⁶J. C. Wooley, B. R. Pamplin, and P. J. Holmes, *J. Less-Common Metals* **1**, 362 (1959).

⁷A. I. Zaslavskii, N. F. Kartenko, and Z. A. Karachentseva, *Fiz. Tverd. Tela* **13**, 2562 (1971) [*Sov. Phys. Solid State* **13**, 2152 (1972)].

⁸V. P. Zhuze, V. M. Sergeeva, and A. I. Shelykh, *Fiz. Tverd. Tela* **2**, 2858 (1960) [*Sov. Phys. Solid State* **2**, 2545 (1961)].

⁹V. A. Petrusevich and V. M. Sergeeva, *Fiz. Tverd. Tela* **2**, 2881 (1960) [*Sov. Phys. Solid State* **2**, 2562 (1961)].

¹⁰Materials preparation and characterization will be

described elsewhere.

¹¹The $(2\pi/a)(1, 1, 0)$ point is equivalent to the $(2\pi/a) \times (1, 0, 0)$ point in the zb BZ. At this point, the transverse modes are doubly degenerate E modes with zero dipole moments and are not infrared active [H. Montgomery, Proc. Roy. Soc., Ser. A **309**, 521 (1969); G. D. Holah, J. Phys. C: Proc. Phys. Soc., London **5**, 1893 (1972)].

¹²J. F. Vetelino, S. S. Mitra, and K. V. Namjoshi, Phys. Rev. B **2**, 967 (1970).

¹³R. H. Parmenter, Phys. Rev. **100**, 573 (1955); J. T.

Birman, Phys. Rev. **131**, 1489 (1963).

¹⁴P. J. Holmes, I. C. Jennings, and J. E. Parrott, J. Phys. Chem. Solids **23**, 1 (1962).

¹⁵We did not observe any polarization effects in the infrared spectra measured on our single crystals of α - In_2Te_3 , but the crystals contained defects.

¹⁶P. C. Newman, J. Phys. Chem. Solids **23**, 19 (1962).

¹⁷L. Patrick, D. R. Hamilton, and W. J. Choyke, Phys. Rev. **143**, 526 (1966); D. W. Feldman, J. H. Parker, Jr., W. J. Choyke, and L. Patrick, Phys. Rev. **173**, 787 (1968).

Direct Optical Excitation of the Surface Photoelectric Effect

S. A. Flodström

Department of Physics and Measurement Technology, Linköping University, Linköping, Sweden

and

J. G. Endriz

RCA Laboratories, David Sarnoff Research Center, Princeton, New Jersey 08540

(Received 12 July 1973)

Measurements on Al of the ratio of the photoyields by p - and s -polarized light, Y_p/Y_s , and the absolute yield for p -polarized light Y_p , at different angles of light incidence and at energies near photoemissive threshold, give results which are in excellent agreement with the strength of the surface photoelectric effect implied in recent calculations.

We present in this paper what we believe to be the first experimental evidence which unambiguously shows the direct optical excitation of the surface photoelectric effect.^{1,2} Excitation of the effect in surface-plasmon decay has recently been reported and explained.³ In contrast, no firm data have previously been presented for direct optical excitation of the effect although the literature of attempts to do so spans three decades.^{1,4,5} This apparent paradox between observation of the surface effect in surface plasmon decay and failure to observe it in direct optical excitation has been in large measure cleared up in a recent theoretical description of the surface photoelectric effect, which stresses the heretofore unappreciated strong frequency dependence in the effect while pointing out the importance which surface roughness can have in any experimental studies.⁶

Briefly stated, the theoretical treatment⁶ points out that the surface effect is strongest near threshold frequencies in nearly free-electron metals, becoming weaker at higher energies, and almost totally suppressed near the volume plasma energy. Because surface plasmons can exist near these threshold energies and are easily excited through slight surface roughness, the

decay of these plasmons introduces strong surface photoexcitation which can severely perturb any photoyield measurements. It is thus suggested that any attempts at direct optical observation of the surface effect be carried out near threshold energies on very smooth samples of metals for which the surface plasma energy is energetically removed from the photoemission threshold (e.g., polyvalent metals).

Aluminum, the metal chosen for the present studies, is almost unique among nearly free-electron metals in having a surface plasma energy (10.5 eV) well removed from its threshold energy (4.1 eV), and in being amenable to smooth-surface preparation.^{3,7} By contrast, most of the previous experimental attempts at observing optical excitation of the surface effect were carried out on the alkali metals at energies for which the surface effect would be expected to be weak, or obscured by spurious coupling to surface plasmons. It is particularly difficult to obtain extremely smooth samples of the alkali metals.

The Al films described in this paper were prepared by evaporation of 1000-Å films in 1 min at pressures of 2×10^{-8} Torr, followed by measurement at 1×10^{-10} Torr. Surface rough-